

# Gaussian Multiple Access Channel with Compact Antenna Arrays

Michel T. Ivrlač and Josef A. Nossek

Institute for Circuit Theory and Signal Processing  
Technische Universität München, D-80333 Munich, Germany  
email: {ivrlac,nossek}@tum.de

**Abstract**—We report on our investigation of the capacity region of a Gaussian multiple access channel with two independent transmitters for the case where the receiver’s antenna spacing is very small (compared to the wavelength). In contrast to common belief, we find that a *rectangular* capacity region can be maintained even as the distance of the antennas *approaches zero*. Moreover, the size of the capacity region even *increases* as the antenna separation is *reduced*. Therefore, high-performance multiple access is perfectly possible in confined space situations such as in hand-held mobile devices using standard frequencies for mobile communications.

## I. INTRODUCTION

In a multiple access channel (MAC), some number of independent transmitters communicate simultaneously with a receiver while using the same band of frequencies. The capacity region of the MAC can be increased if the receiver uses multiple antennas [1]. Consider, for instance, the Gaussian MAC with two independent single-antenna transmitters, where

$$\mathbb{C}^N \ni \mathbf{y} = \mathbf{h}_1 x_1 + \mathbf{h}_2 x_2 + \mathbf{n} \quad (1)$$

is the received signal vector,  $\mathbf{n} \sim \mathcal{CN}(\mathbf{0}, \sigma_n^2 \mathbf{I})$  is additive white Gaussian noise (AWGN),  $x_1$  and  $x_2$  are the independent Gaussian transmit signals, while  $\mathbf{h}_1$  and  $\mathbf{h}_2$  are the  $N$ -dimensional channel vectors, where  $N$  is the number of receiver antennas. Assuming that the receiver knows the channel vectors  $\mathbf{h}_1$  and  $\mathbf{h}_2$ , it is possible that the capacity region of this MAC has got *rectangular* shape. This happens *only* when  $\mathbf{h}_2^H \mathbf{h}_1 = 0$ , that is, when the channel vectors are (by chance) *orthogonal*. When the capacity region is rectangular, each transmitter can achieve the same rate as it could have achieved if it had the channel only to itself. This is the best situation for independent transmitters. Of course, all of this is well known.

The contribution of this paper is the analysis of what actually happens when the distance between the antennas inside the receiver’s array becomes small compared to the wavelength and, ultimately, is reduced towards zero. In this extreme case, the antennas are almost at the same position in space, forming something that might be called a »point-array«. It seems fairly natural that all the antennas of the point-array should sample essentially the *same* electric field, for they are located almost at the *same* position in space. Therefore, the channel vectors  $\mathbf{h}_1$  and  $\mathbf{h}_2$  should converge to scaled *all-ones* vectors when the antenna separation is reduced towards zero. Obviously, in this case the channel vectors are not orthogonal any more, in fact they are co-linear. As a result, the capacity region cannot be rectangular anymore when the antennas are placed very densely. All this seems quite intuitive. Only, is it true?

The trouble with this standard argument given above is that it ignores the electromagnetic interaction of closely spaced an-

tennas. Electric currents flowing in each antenna excite electromagnetic fields of their own which are felt and responded to by neighboring antennas. For small antenna separation (compared to the wavelength) this leads to strong mutual near-field coupling. These electrodynamic effects turn out to have profound influence on the information theoretic capabilities of the communication system.

In this paper, we show that the MAC channel vectors actually *can be orthogonal* despite the antenna separation being reduced towards zero (with respect to the wavelength). Thus, *the capacity region of the resulting Gaussian MAC actually can be rectangular, no matter how compactly the receiver antennas are spaced*. Moreover, it turns out that the Gaussian MAC capacity region employing dense arrays is *strictly larger* than that for the more usual case of widely spaced antennas. These results indicate that the size of the receiver’s antenna array does *not* limit the information theoretic capability of the resulting MAC. This has practical implications for confined space situations like in mobile hand-held devices, indicating the capability to deliver excellent multi-antenna MAC performance at standard frequencies employed in current mobile communications.

## II. SYSTEM UNDER CONSIDERATION

Consider the system shown schematically in Figure 1, displaying two independent transmitters (Tx1 and Tx2), and a receiver which uses  $N = 4$  antennas (labeled 1, 2, 3, and 4), positioned uniformly on a circle with the diameter  $d$ . The transmitters have the same distance to the center of the receiver array and are located in the direction of the azimuthal angles  $\phi_0$ , and  $\phi_0 + \pi/2$ , such that the line segments which connect the transmitters with the center of the array form a right angle. We assume that all antennas are *Hertzian dipoles* which

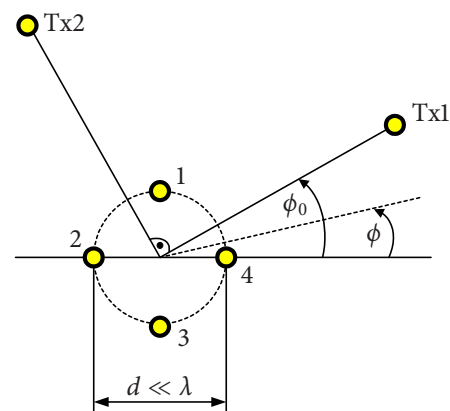


Figure 1: MAC formed by two independent transmitters (Tx1, Tx2), and a compact 4-antenna receiver in empty space.

are *polarized perpendicularly to the drawing plane* in Figure 1. They reside within otherwise empty space, which accounts for a line of sight (LOS) situation.

### III. THE CAPACITY REGION

From an information theory perspective, the system from Figure 1 is a MAC described by (1). For the sake of simplicity, we assume in the following that the same transmit power  $P_T$  is used by the two independent transmitters, such that:

$$[x_1 \ x_2] \sim \mathcal{CN}(\mathbf{0}, P_T \mathbf{I}). \quad (2)$$

When the noise is Gaussian and white with variance  $\sigma_n^2$ , the capacity region of this Gaussian MAC is completely specified by the following three inequalities [1]:

$$0 \leq R_k \leq \log_2 \left( 1 + \frac{P_T}{\sigma_n^2} \|\mathbf{h}_k\|_2^2 \right), \quad k \in \{1, 2\}, \quad (3)$$

$$R_1 + R_2 \leq \log_2 \det \left( \mathbf{I} + \frac{P_T}{\sigma_n^2} \mathbf{H}^H \mathbf{H} \right), \quad \mathbf{H} = [\mathbf{h}_1 \ \mathbf{h}_2]. \quad (3a)$$

Note that (3a) can also be expressed as:

$$\begin{aligned} R_1 + R_2 &\leq \log_2 \left( 1 + \frac{P_T}{\sigma_n^2} \|\mathbf{h}_1\|_2^2 \right) + \\ &+ \log_2 \left( 1 + \frac{P_T}{\sigma_n^2} \|\mathbf{h}_2\|_2^2 - \left( \frac{P_T}{\sigma_n^2} \right)^2 \frac{|\mathbf{h}_2^H \mathbf{h}_1|^2}{1 + \frac{P_T}{\sigma_n^2} \|\mathbf{h}_1\|_2^2} \right). \end{aligned} \quad (4)$$

From (4) it is clear that *only* in the case that  $\mathbf{h}_2^H \mathbf{h}_1 = 0$ , the inequality (3a) is redundant, for it is fulfilled whenever (3) are fulfilled. Thus, if and only if the channel vectors are orthogonal, the capacity region has the shape of a rectangle, defined by (3). To compute the capacity region for the system from Figure 1, we have to determine the channel vectors  $\mathbf{h}_1$  and  $\mathbf{h}_2$ .

#### A. Ignoring the Mutual Coupling

The standard way of determining the channel vectors  $\mathbf{h}_1$  and  $\mathbf{h}_2$  *ignores* electromagnetic interaction between antennas and the electromagnetic field. Following this standard approach [1], the channel vectors are described by the *array steering vectors*, which are found for the geometry from Figure 1 as:

$$\mathbf{a}(\phi) = \begin{bmatrix} \exp(j\pi(d/\lambda) \sin \phi) \\ \exp(-j\pi(d/\lambda) \cos \phi) \\ \exp(-j\pi(d/\lambda) \sin \phi) \\ \exp(j\pi(d/\lambda) \cos \phi) \end{bmatrix}, \quad (5)$$

with the array center taken as phase reference. Herein,  $\lambda$  is the wavelength, and  $\phi$  the azimuthal angle of an impinging planar wavefront (see Figure 1). Ignoring mutual antenna coupling, the channel vectors become (see [1], page 297):

$$\mathbf{h}_1 = \alpha \mathbf{a}(\phi_0), \quad \mathbf{h}_2 = \alpha \mathbf{a}(\phi_0 + \pi/2), \quad (6)$$

where  $\alpha$  is a complex valued constant. Because of

$$\mathbf{h}_2^H \mathbf{h}_1 = |\alpha|^2 e^{j\gamma} \left( 1 + e^{j2\pi \frac{d}{\lambda} \cos \phi_0} \right) \left( 1 + e^{j2\pi \frac{d}{\lambda} \sin \phi_0} \right), \quad (7)$$

where  $\gamma = -\pi \frac{d}{\lambda} (\cos(\phi_0) + \sin \phi_0)$ , it is clear that:

$$d/\lambda < \frac{1}{2} \implies \neg \exists \phi_0 : \mathbf{h}_2^H \mathbf{h}_1 = 0. \quad (8)$$

That is, when the diameter  $d$  of the receiver array becomes smaller than half a wavelength, the two channel vectors cannot be orthogonal anymore. This means that for too small a size of the receiver array, the capacity region cannot have the desirable rectangular shape anymore. Now, there is:

$$\|\mathbf{h}_1\|_2^2 = \|\mathbf{h}_2\|_2^2 = 4|\alpha|^2, \quad (9)$$

independent of  $d/\lambda$  and  $\phi_0$ . Moreover,

$$\lim_{d/\lambda \rightarrow 0} \mathbf{h}_2^H \mathbf{h}_1 = 4|\alpha|^2. \quad (10)$$

Fixing the transmit power to the value:

$$P_T = \frac{\sigma_n^2}{4|\alpha|^2}, \quad (11)$$

one then obtains with the help of (3) and (4) that the capacity region of the *point-array* is given by:

$$d/\lambda \rightarrow 0 \implies 0 \leq R_{1,2} \leq 1, \quad R_1 + R_2 \leq \log_2 3. \quad (12)$$

Recall that these results are based on the assumption that there is *no* mutual coupling between the very closely spaced antennas. This is, of course, *not* consistent with the electromagnetic theory. Hence, the result (12) makes no sense from a physics perspective. Let us now see what *actually* happens.

#### B. Taking Mutual Coupling into Account

To regain consistency with the governing physics, one has to take the mutual antenna coupling fully into account. In the next Section we will do just that, thereby showing:

$$\lim_{d/\lambda \rightarrow 0} \|\mathbf{h}_1\|_2^2 = \lim_{d/\lambda \rightarrow 0} \|\mathbf{h}_2\|_2^2 = |\alpha|^2 \frac{17 + 5 \cos 4\phi_0}{24/7}. \quad (13)$$

In contrast to (9), the squared Euclidean norm of the channel vectors *does* depend on the angle  $\phi_0$  (see Figure 1). The largest norm occurs when  $\phi_0$  is an integer multiple of  $90^\circ$ . Its value of about  $6.4|\alpha|^2$  is also significantly larger than the prediction from (9) which did not take the mutual coupling into account. What is even more remarkable, however, is that:

$$\lim_{d/\lambda \rightarrow 0} \mathbf{h}_2^H \mathbf{h}_1 = -|\alpha|^2 \frac{11 + 35 \cos 4\phi_0}{24}. \quad (14)$$

Therefore, the channel vectors *actually can be orthogonal*. E.g.,

$$\phi_0 = \frac{1}{4} \arccos \frac{-11}{35} \approx 27^\circ \implies \lim_{d/\lambda \rightarrow 0} \mathbf{h}_2^H \mathbf{h}_1 = 0. \quad (15)$$

Using this value for  $\phi_0$  in (13) it follows with the help of (15), (11), (3) and (4), that the *actual* capacity region for the point array is given by:

$$d/\lambda \rightarrow 0, \quad \phi_0 = \frac{1}{4} \arccos \frac{-11}{35} \implies 0 \leq R_{1,2} \leq \log_2 \frac{17}{8}. \quad (16)$$

That is, the capacity region of a MAC with an arbitrarily small array can indeed be *rectangular*. Comparing (16) with (12), the actual capacity region is larger than predicted without taking mutual antenna coupling into account. Figure 2 shows a graph-

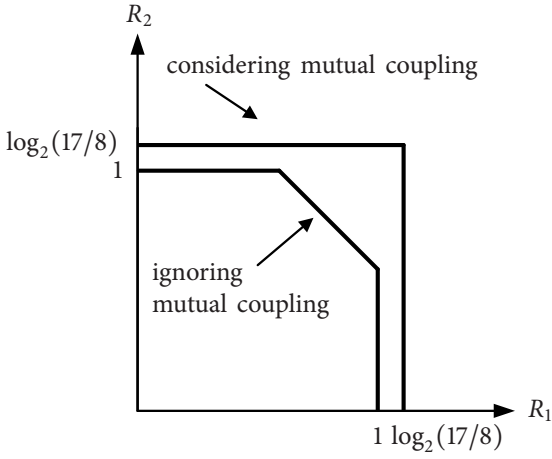


Figure 2: Capacity region for the MAC from Figure 1 using a point-array ( $d/\lambda \rightarrow 0$ ), for the cases where mutual antenna coupling is either considered [(16)], or ignored [(12)].

ical representation of the MAC capacity regions for the point array, which result either from considering the mutual coupling (see (16)), or from ignoring mutual coupling (see (12)). Note that taking the mutual antenna coupling into account not only makes the result consistent with electromagnetic theory, but also reveals that the performance of the point-array is *better* than predicted from ignoring mutual coupling.

#### IV. DEALING WITH MUTUAL ANTENNA COUPLING

In the following, we show how to obtain the results (13) and (14) claimed in the previous Section. To do this, we need to find a way how to take the mutual antenna coupling into account. In general, this can be done using multiport theory [2]–[4]. Hereby, the receiver's array of four antennas is modeled as a linear electric four-port. Each port is characterized by two physical quantities: namely a port voltage and a port current. Due to linearity, the relationships among these eight port variables are completely described by the array's impedance matrix  $\mathbf{Z}_A \in \mathbb{C}^{4 \times 4} \cdot \Omega$ , and the help of one voltage source in series at each port, such that the vector  $\mathbf{u}_A = [u_{A,1} \ u_{A,2} \ u_{A,3} \ u_{A,4}]^T$  of the antenna port voltages can be written as:

$$\mathbf{u}_A = \mathbf{Z}_A \mathbf{i}_A + \mathbf{u}_S + \tilde{\mathbf{u}}_N, \quad (17)$$

wherein  $\mathbf{u}_S = [u_{S,1} \ u_{S,2} \ u_{S,3} \ u_{S,4}]^T$  is the vector of the voltages which appear at the *open-circuited* ports as a result of the impinging wavefronts which originate from the two transmitters. The vector  $\tilde{\mathbf{u}}_N = [\tilde{u}_{N,1} \ \tilde{u}_{N,2} \ \tilde{u}_{N,3} \ \tilde{u}_{N,4}]^T$  is the vector of *open-circuit* noise voltages received by the antenna, while the vector  $\mathbf{i}_A = [i_{A,1} \ i_{A,2} \ i_{A,3} \ i_{A,4}]^T$  contains the antenna port currents. When the background noise impinges on the antenna array *isotropically*, it can be shown [5] that the noise voltage vector

$$\tilde{\mathbf{u}}_N \sim \mathcal{CN}(\mathbf{0}, 4kT_A \Delta f \operatorname{Re}\{\mathbf{Z}_A\}), \quad (18)$$

where  $k$  is the Boltzmann constant,  $T_A$  is the *noise temperature* [6] of the antennas, and  $\Delta f$  is the bandwidth. As is shown in Figure 3, the noisy antenna ports are connected to the inputs

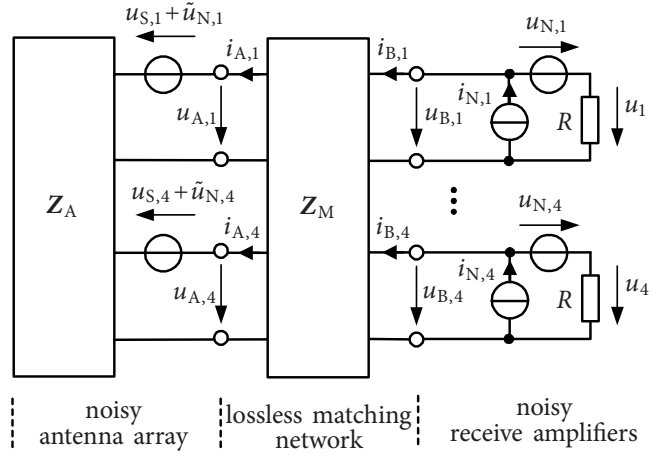


Figure 3: Multiport model of a noisy antenna array connected to noisy receive amplifiers via a lossless matching multiport. The observable outputs are the voltages  $u_1, \dots, u_4$ .

of a *matching network*, which operation shall be described by:

$$\begin{bmatrix} \mathbf{u}_B \\ \mathbf{u}_A \end{bmatrix} = \mathbf{Z}_M \begin{bmatrix} \mathbf{i}_B \\ -\mathbf{i}_A \end{bmatrix}. \quad (19)$$

Here,  $\mathbf{u}_B = [u_{B,1} \ u_{B,2} \ u_{B,3} \ u_{B,4}]^T$  and  $\mathbf{i}_B = [i_{B,1} \ i_{B,2} \ i_{B,3} \ i_{B,4}]^T$  are the vectors of the port voltages and port currents at the matching networks' output. Elementary analysis of the circuit in Figure 3 shows that choosing the impedance matrix

$$\mathbf{Z}_M = \begin{bmatrix} j \operatorname{Im}\{\mathbf{Z}_{\text{out}}\} \mathbf{I} & j \sqrt{\operatorname{Re}\{\mathbf{Z}_{\text{out}}\}} \operatorname{Re}\{\mathbf{Z}_A\}^{1/2} \\ j \sqrt{\operatorname{Re}\{\mathbf{Z}_{\text{out}}\}} \operatorname{Re}\{\mathbf{Z}_A\}^{1/2} & -j \operatorname{Im}\{\mathbf{Z}_A\} \end{bmatrix}, \quad (20)$$

ensures that the output ports of the matching network become electrically *decoupled* and present to the receive amplifiers the output impedance  $Z_{\text{out}}$ . Note that (20) defines a purely imaginary symmetric matrix. This means that the matching network is a *lossless and reciprocal* multiport [2]. The noisy receive amplifiers are modeled in the usual way [7] by representing them by their input resistance  $R$ , a noise voltage source  $u_{N,j}$ , and a noise current source  $i_{N,j}$ , with  $j \in \{1, \dots, 4\}$ . Because the four receive amplifiers are independent devices, it is reasonable to assume that the noise contributions of different amplifiers are uncorrelated. The system's output is collected into the vector  $\mathbf{u} = [u_1 \ u_2 \ u_3 \ u_4]^T$  of the noisy observable voltages shown on the right-most end of Figure 3. From circuit analysis follows

$$\mathbf{u} = \frac{jR \sqrt{\operatorname{Re}\{\mathbf{Z}_{\text{out}}\}}}{R + Z_{\text{out}}} \operatorname{Re}\{\mathbf{Z}_A\}^{-1/2} \mathbf{u}_S + \mathbf{n}, \quad (21)$$

where  $\mathbf{n} \in \mathbb{C}^{4 \times 1} \cdot V$  is the total noise voltage vector with

$$\mathbf{n} \sim \mathcal{CN}(\mathbf{0}, \sigma_n^2 \mathbf{I}). \quad (22)$$

Because of the operation of the lossless matching network, the resulting observed noise is indeed *white* and Gaussian. It can be shown that its variance  $\sigma_n^2$  is *independent* of the diameter  $d/\lambda$  of the antenna array [4]. What remains to be found is the signal voltage vector  $\mathbf{u}_S$ , and the real-part of the impedance matrix  $\mathbf{Z}_A$ . Because the Hertzian dipoles do not disturb the electromagnetic field when the port currents vanish [3], [8],

the *open-circuit* voltage vector  $\mathbf{u}_S$  which results from an impinging planar wavefront is proportional to the array steering vector (5) corresponding to the wavefront's direction  $\phi$  of arrival. For the 2 transmitter scenario from Figure 1, this means:

$$\mathbf{u}_S = \beta \mathbf{a}(\phi_0)x_1 + \beta \mathbf{a}(\phi_0 + \pi/2)x_2, \quad (23)$$

where  $\beta$  is some complex valued scalar constant, and  $x_1$  and  $x_2$  are the information carrying transmit signals from (2). Substituting (23) into (21), we obtain:

$$\mathbf{u} = \gamma \text{Re}\{\mathbf{Z}_A\}^{-1/2} \mathbf{a}(\phi_0)x_1 + \gamma \text{Re}\{\mathbf{Z}_A\}^{-1/2} \mathbf{a}(\phi_0 + \pi/2)x_2 + \mathbf{n}, \quad (24)$$

where  $\gamma = j\beta R \sqrt{\text{Re}\{Z_{\text{out}}\}} / (R + Z_{\text{out}})$  is yet another scalar constant. Now for the real-part of the array's impedance matrix. For two parallel Hertzian dipoles spaced a distance  $s$  apart, it can be shown (see [8], [9]) that

$$N = 2 \quad \longrightarrow \quad \text{Re}\{\mathbf{Z}_A\} = R_r \begin{bmatrix} 1 & \Psi(ks) \\ \Psi(ks) & 1 \end{bmatrix}, \quad (25)$$

where  $R_r$  is the radiation resistance of the Hertzian dipole [3],  $k = 2\pi/\lambda$ , and

$$\Psi(x) = \frac{3}{2} \left( \frac{\sin x}{x} + \frac{\cos x}{x^2} - \frac{\sin x}{x^3} \right). \quad (26)$$

In the array shown in Figure 1, there are two possible distances between antenna pairs, namely  $d$  and  $d/\sqrt{2}$ . Hence, generalizing (25) to the  $N = 4$  antenna array from Figure 1, we obtain:

$$\text{Re}\{\mathbf{Z}_A\} = R_r \mathbf{C}, \quad (27)$$

where

$$\mathbf{C} = \begin{bmatrix} 1 & \Psi(kd/\sqrt{2}) & \Psi(kd) & \Psi(kd/\sqrt{2}) \\ \Psi(kd/\sqrt{2}) & 1 & \Psi(kd/\sqrt{2}) & \Psi(kd) \\ \Psi(kd) & \Psi(kd/\sqrt{2}) & 1 & \Psi(kd/\sqrt{2}) \\ \Psi(kd/\sqrt{2}) & \Psi(kd) & \Psi(kd/\sqrt{2}) & 1 \end{bmatrix}. \quad (28)$$

When the Hertzian dipoles are replaced by thin  $\lambda/2$  dipoles, it turns out that the matrix  $\mathbf{C}$  from (28) comes out essentially the same. When we identify the output vector  $\mathbf{y}$  from (1) with the voltage vector  $\mathbf{u}$  from (24), it follows with the help of (27) and (28) that the channel vectors from (1) are given by:

$$\mathbf{h}_1 = \alpha \mathbf{C}^{-1/2} \mathbf{a}(\phi_0), \quad \mathbf{h}_2 = \alpha \mathbf{C}^{-1/2} \mathbf{a}(\phi_0 + \pi/2), \quad (29)$$

where  $\alpha = \gamma R_r$  is a scalar constant. Comparing (29) with (6), it is clear that ignoring mutual antenna coupling corresponds to setting the matrix  $\mathbf{C}$  in (29) equal to the identity matrix, while, in fact, it is given by (28). Note that, as  $d/\lambda \rightarrow 0$ , the matrix  $\mathbf{C}$  approaches the all-ones matrix. Substituting (5) and (28) into (29) one finally obtains that:

$$\lim_{d/\lambda \rightarrow 0} \mathbf{h}_1 = \alpha \begin{bmatrix} a & b & a^* & b^* \end{bmatrix}^T, \quad \lim_{d/\lambda \rightarrow 0} \mathbf{h}_2 = \alpha \begin{bmatrix} b^* & a & b & a^* \end{bmatrix}^T, \quad (30)$$

where

$$a = (6 + \sqrt{105} \cos(2\phi_0) + j6\sqrt{5} \sin \phi_0) / 12, \quad (31)$$

$$b = (6 - \sqrt{105} \cos(2\phi_0) - j6\sqrt{5} \cos \phi_0) / 12. \quad (31a)$$

The claims (13) and (14) then follow immediately from (30), (31) and (31a). The computation of the inverse matrix square root  $\mathbf{C}^{-1/2}$  can be carried out by means of an eigenvalue decomposition of  $\mathbf{C}$ . In Figure 4, the capacity regions of the

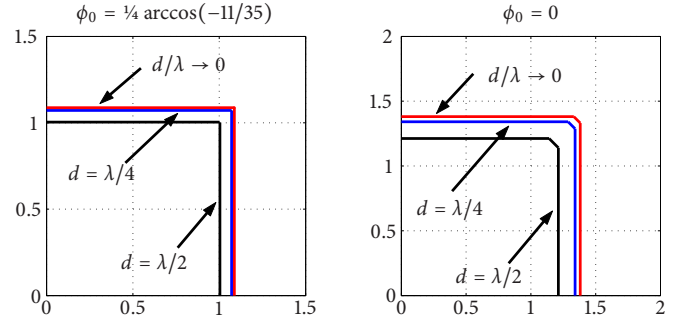


Figure 4: Actual capacity regions for the MAC from Figure 1 when mutual antenna coupling is taken into account, for three different diameters of the antenna array, and two different user positions ( $\phi_0 \in \{ \frac{1}{4} \arccos(-11/35), 0 \}$ ).

MAC from Figure 1 are shown for different sizes of the antenna array and different transmitter positions. They are computed by substituting (5) and (28) into (29), and the latter into (3) and (3a), while the transmit power is held constant (see (11)) in all cases. Note that the MAC employing the point-array ( $d/\lambda \rightarrow 0$ ) offers a *strictly larger* capacity region than the MACs with larger arrays. This result is true not only for the two user positions shown in Figure 4, but for all user positions  $\phi_0 \in [0, 2\pi]$ .

## V. CONCLUSION

A compact size of the receiver's antenna array does *not* impair the capacity region of a Gaussian multiple access channel. On the contrary, it is the *smallest* arrays (much smaller than half the wavelength) which offer the *largest* capacity region for the same transmit power. This perhaps counter-intuitive result is a consequence of the physics of mutual electromagnetic antenna coupling in conjunction with a properly engineered matching network. In contrast to folklore belief, compact antenna arrays make attractive candidates for excellent multiple access performance in confined-space situations, like in mobile handsets.

## REFERENCES

- [1] D. Tse and P. Viswanath, *Fundamentals of Wireless Communication*. Cambridge University Press, 2005.
- [2] V. Belevitch, *Classical Network Theory*. Holden Day, San Francisco, 1968.
- [3] A. Balanis, *Antenna Theory*. Second Edition, John Wiley & Sons, 1997.
- [4] M. T. Ivrlač and J. A. Nossek, "Toward a Circuit Theory of Communication," *IEEE Transactions on Circuits and Systems I: Regular Papers*, vol. 57(7), pp. 1663–1683, 2010.
- [5] R. Q. Twiss, "Nyquist's and Thevenin's Theorems Generalized for Nonreciprocal Linear Networks," *Journal of Applied Physics*, vol. 26, pp. 599–602, May 1955.
- [6] K. F. Warnick, E. E. Woestenburger, L. Belostotski, and P. Russer, "Minimizing the Noise Penalty Due to Mutual Coupling for a Receiving Array," *IEEE Transactions on Antennas and Propagation*, vol. 57(6), pp. 1634–1644, jun 2009.
- [7] H. Hillbrand and P. Russer, "An Efficient Method for Computer Aided Noise Analysis of Linear Amplifier Networks," *IEEE Transactions on Circuits and Systems*, vol. 23(4), pp. 235–238, jun 1976.
- [8] S. A. Schelkunoff and H. T. Friis, *Antennas. Theory and Practice*. New York, NY: Wiley, 1952.
- [9] H. Yordanov, M. T. Ivrlač, P. Russer, and J. A. Nossek, "Arrays of Isotropic Radiators — A Field-theoretic Justification," in *Proc. of the IEEE/ITG International Workshop on Smart Antennas, 2009*, Berlin, Germany, feb 2009.